Enhanced Harmonic Generation from Expanding Clusters

B. Shim, G. Hays, R. Zgadzaj, T. Ditmire, and M. C. Downer*

FOCUS Center, Department of Physics, University of Texas at Austin, Austin, Texas 78712-1081, USA

(Received 6 July 2006; published 20 March 2007)

We report controlled enhancement of optical third harmonic generation (THG) from hydrodynamically expanding clusters of $\sim 6 \times 10^5$ noble-gas atoms several hundred femtoseconds following ionization and heating by ultrashort pump pulses. This resonant enhancement is more pronounced for orthogonal than for parallel pump-probe polarizations, a consequence of faster cluster expansion along the pump polarization. Simulations show that the nonlinear susceptibility $\chi^{(3)}$ of the individual clusters and the coherence length of the clustered plasma medium are optimized nearly simultaneously as the clusters expand, and both contribute to the observed THG enhancement. This dual enhancement mechanism may be scalable to relativistic probe intensity and to generation of high-order harmonics in the soft-x-ray regime.

DOI: 10.1103/PhysRevLett.98.123902 PACS numbers: 42.65.Ky, 32.80.Wr, 36.40.Gk

Harmonic generation (HG) by intense ultrashort laser pulses interacting with gas [1] or solid [2] targets can produce coherent, collimated radiation from near ultraviolet to soft-x-ray wavelengths with pulse durations down to the attosecond regime [3]. The low energy of the short-wavelength pulses, however, has inhibited widespread applications and spurred continuing research into improving conversion efficiency. Clustered gases provide a hybrid nonlinear medium with local solid density, but global gas density, that can combine the advantages of gas targets (extended interaction length, possibility of phase-matching [4]) and solid targets (high saturation intensity, large nonlinear susceptibility $\chi^{(n)}$, control via preexpansion) for harmonic generation. Donnelly *et al.* [5] first observed that harmonics from atomic clusters in a high-pressure gas jet could be generated to higher order and with less saturation than from a monomer gas jet, but overall efficiency enhancement, and methods to control it, were lacking. Subsequently, clustered plasmas were proposed as a unique nonlinear medium in which both phase-matching [6] and resonantly-enhanced odd-order ($n = 3, 5, \ldots$) $\chi^{(n)}$ [7,8] could be achieved at selected cluster sizes and densities. However, experiments have not yet realized these possibilities. Controlled resonance enhancement of the complex linear susceptibility $\chi^{(1)}$ was demonstrated [9,10] by preexpanding clusters with an ionizing or heating pulse and explained using models of expanding clustered plasma [11,12]. This result suggested a path to controlled enhancement of nth-order harmonic generation since $\chi^{(n)}$ undergoes analogous resonant enhancement during cluster expansion [7,8], while simultaneous variations in $\chi^{(1)}$ can potentially optimize phase matching.

In this Letter, we report enhanced third-harmonic generation (THG) from a plasma of rapidly expanding noble-gas clusters. A pump generates the clustered plasma, composed of ionized clusters and residual coronal plasma, in a gas jet and initiates cluster expansion. A probe then generates third-harmonic (TH) radiation at controlled time delays Δt. We observe a sharp enhancement of probe-generated TH radiation at time delays $150 < \Delta t < 350$ fs preceding, and more localized in time than the $\chi^{(1)}$ resonance. Analysis shows that resonant $\chi^{(3)}$ enhancement of individual clusters and increased coherence length in the macroscopic clustered medium both contribute to the observed enhancement. The resonant enhancement is more pronounced for orthogonal than for parallel pump-probe polarizations, a consequence of the transient anisotropy of cluster hydrodynamic expansion [13,14]. The linear optical response, by contrast, is isotropic. The physical mechanisms contributing to enhanced THG may be scalable to relativistic probe intensity and to high-order harmonic generation.

For experiments, 800 nm, 100 fs, $\sim$0.1 J pulses from a 10 Hz Ti:sapphire laser system were split into pump and probe beams. Second-harmonic pump pulses (400 nm, 100 fs) were generated in a 1 mm thick, type-I KDP crystal; the remaining 800 nm beam served as the probe. A $\lambda/2$ plate and thin polarizer adjusted probe energy and polarization. A translation stage controlled pump-probe delay. Clusters formed in a pulsed supersonic Ar gas jet emanating from a 750 μm diameter orifice with 11° half expansion angle backed with 600 psi argon. Under these conditions, $\sim$20% of the Ar atoms condensed into clusters of 20 nm average radius while the rest remained as monomers [15]. Pump and probe were focused into the jet by separate singlet lenses to beam diameters ($1/e^2$) 40 μm and 30 μm, respectively, and combined by a dichroic beam splitter. Peak pump intensity was maintained at $I_{\text{pump}} = 10^{15}\ \text{W/cm}^2$, while probe intensity was varied over the range $2 \times 10^{13} \leq I_{\text{probe}} \leq 8 \times 10^{15}\ \text{W/cm}^2$. Nonlinear interactions in the jet generated the third-harmonic $E^{3\omega}_{\text{THG}} \propto \chi^{(3)}(E^{\omega}_{\text{probe}})^3$ of the probe at all Δt, and a Four-Wave Mixing (FWM) signal $E^{3\omega}_{\text{FWM}} \propto \chi^{(3)}(E^{\omega}_{\text{probe}})^*(E^{2\omega}_{\text{pump}})^2$ at the same frequency when pump and probe overlapped in time. To separate these signals, we intersected pump and probe at a small angle ($\sim$2°), so that THG and FWM

signals propagated in different directions governed by momentum conservation. The FWM signal was then blocked after the interaction region. Pump and probe passed through an off-center chord of the circular gas jet profile 2.5 mm from the nozzle, with path length $L \approx 1$ mm matched to the length of the pump-probe overlap region. In this configuration probe defocusing by its self-created plasma lens, and pump-induced probe refraction [10,16], were both negligible. A Mach-Zehnder interferometer measured average atomic density $\sim 10^{18}$ cm^{-3}. An $f/4$ lens collected TH signal into a spectrometer for spectral discrimination and detection. Time-resolved probe absorption was also measured through a red glass filter with an energy meter.

Figure 1 contrasts the time evolution of probe THG and absorption when the probe was weak (2×10^{13} W/cm^2) and polarized parallel to the pump. A sharp enhancement of THG occurred at $\Delta t \sim -100$ fs, when the leading edge of the pump ionized the clusters, sweeping the plasma frequency ω_p in the cluster rapidly upward through the resonant condition $\alpha\omega_p = 3\omega$, where α is a geometrical factor equal to $1/\sqrt{3}$ for a spherical plasma [17]. Although a weak corresponding resonance at $\Delta t < 0$ can be discerned in calculated linear absorption (solid curve in Fig. 1, discussed below), it was too weak to observe, evidently because $\alpha\omega_p$ swept upward through ω rapidly compared to a collision period. On the other hand, a prominent delayed absorption resonance was observed at $\Delta t \sim 400$ fs, and lasted 2 to 3 ps, as $\alpha\omega_p$ dropped slowly back through ω as the cluster expanded. However, no THG resonance was observable at $\Delta t > 0$. Instead, THG became weaker than from the nonionized medium.

As I_{probe} increased, the peak at $\Delta t < 0$ saturated [Fig. 2(a), left], and a delayed THG peak at $\Delta t \sim 260$ fs appeared and rapidly grew to $>5\times$ the level at negative delays [Fig. 2(a), right]. The former peak scaled as I^3_{probe} when $I_{\text{probe}} < 10^{14}$ W/cm^2 (Ar ionization threshold), but saturated as probe self-ionization became significant [Fig. 2(b)]. The delayed peak, by contrast, scaled as I^3_{probe} without saturation up to $I_{\text{probe}} \approx I_{\text{pump}} \approx 10^{15}$ W/cm^2 [Fig. 2(c)]. As I_{probe} exceeded I_{pump}, the probe further ionizes the monomer plasma, thus decreasing THG coherence length and causing the observed saturation. The delayed peak corresponds to $\alpha\omega_p = 3\omega$ during cluster expansion and thus precedes the absorption resonance at $\alpha\omega_p = \omega$. The delayed THG peak terminates abruptly at $\Delta t > 300$ fs as probe absorption sharply rises. We ruled out the possibility that the delayed THG peak was caused by pump-induced probe focusing [16], and thus increased I_{probe}, by imaging the probe mode from the gas jet exit onto a CCD camera. Probe mode diameter changed by $<10\%$ at any Δt. Taking into account increased probe absorption, I_{probe} actually decreased $\sim 2\times$ from $\Delta t = 0$ to $\Delta t = 300$ fs. The observed THG enhancement must therefore be attributed to an increase in $\chi^{(3)}$ and/or the coherence length of THG. No THG or absorption enhancement was observed in an unclustered He jet of equivalent average atomic density, demonstrating that expanding clusters caused the observed enhancements.

When probe polarization was turned perpendicular to the pump, the delayed THG peak doubled in amplitude (see Fig. 3), yet THG remained isotropic for $\Delta t < 0$ (unexpanded clusters) and $\Delta t \gtrsim 600$ fs (approaching uniform plasma). Anisotropic $\chi^{(3)}$ responses have been observed previously in unclustered plasmas [18]. Here, transient THG anisotropy is qualitatively consistent with observations of anisotropic ion and electron emission from large

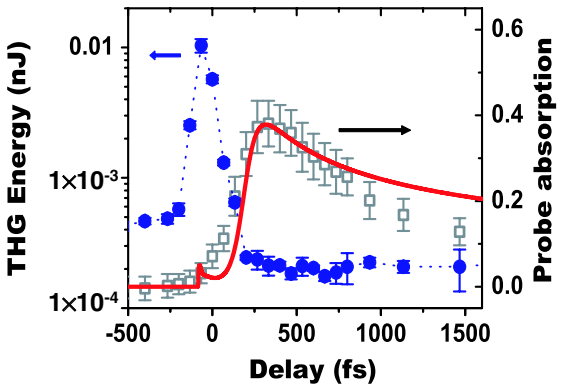

FIG. 1 (color online). THG (filled circles) by and absorption (open squares) of a weak probe (2×10^{13} W/cm^2) following pump excitation at 10^{15} W/cm^2 with parallel pump and probe polarization. Identical absorption is observed with orthogonal polarizations. Solid curve is calculated from uniform density model; dashed curve guides the eye. Each data point represents a 300 shot average.

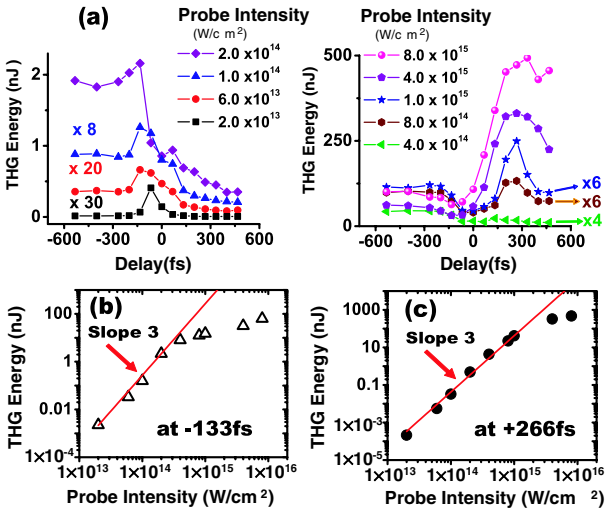

FIG. 2 (color online). (a) Time-dependent, probe THG from clustered Ar jet for pump intensity 10^{15} W/cm^2, for various probe intensities with parallel pump-probe polarizations. Lower panels: I_{probe}-dependence of (b) early THG peak and (c) delayed THG peak, compared to I^3_{probe}.

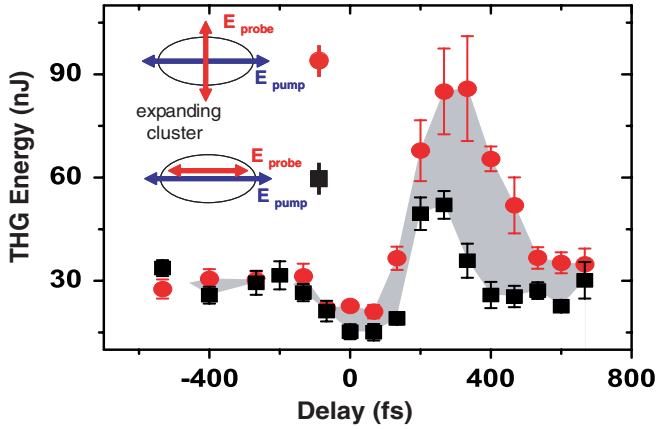

FIG. 3 (color online). Anisotropy of THG from expanding clusters, with pump and probe both at 10^{15} W/cm^2 with parallel (filled squares) or perpendicular (filled circles) polarizations. Each THG data point represents a 100 shot average. Gray shading highlights the region of transient anisotropy.

clusters in both laboratory [13] and simulations [14,19]. While THG and electron- and ion-emission anisotropy may differ in time scale [13] and microscopic origin [14,19], both are consistent with faster cluster elongation along the pump polarization (see Fig. 3 inset). The resulting stronger gradients in ion and electron density transverse to the pump can enhance HG [14,20] for orthogonal pump and probe polarization. This configuration should also be optimum for higher-order HG. Femtosecond pump-probe HG fully time resolves transient cluster anisotropy and is uniquely capable of observing it in clustered plasmas of densities $\gtrsim 10^{18}$ cm^{-3} required for applications to waveguiding [21], nuclear fusion [22], and x-ray generation [23], but too dense for ions or electrons to escape. We observed no anisotropy in time-resolved linear absorption, nor a linear Kerr effect (pump-induced rotation of probe polarization), within experimental error. This illustrates a general principle of nonlinear optics that HG more sensitively probes material anisotropy than linear optics [24].

To interpret the results, we first calculated cluster hydrodynamics and linear optical response using the uniform density model [25]. This model avoids the computational intensity of hydrodynamic [12] or particle [20] simulations by assuming uniform density within the expanding cluster, while empirically modifying electron-ion collisional frequency ν and cluster ion mass to match observed temporal evolution of linear absorption. Laser-cluster interaction was described by field [26] and collisional ionization, inverse bremsstrahlung heating, and hydrodynamic expansion, following Refs. [11,25]. Expansion anisotropy was not included, so $\alpha = 1/\sqrt{3}$. Monomers were field-ionized [26]. The solid curve in Fig. 1 shows an example of calculated probe absorption $1 - \exp(-\alpha_{\rm abs} L)$, where $\alpha_{\rm abs} = 2(k_\omega)(2\pi n_c Im(\frac{\varepsilon_c - 1}{\varepsilon_c + 2}) r_c^3)$ is the absorption coefficient for 800 nm. The ratio of monomer/cluster density was varied (maintaining fixed total atomic density 10^{18} cm^{-3}) to fit the overall magnitude (independent of temporal shape) of time-resolved absorption. The result (0.85 ± 0.05 monomers) agreed with Ref. [15] for our jet conditions and yielded a good fit of observed absorption for $\Delta t \lesssim 1$ ps (see, e.g., Fig. 1). Using parameters from this fit, we then derived refractive indices $n_{\rm jet}(q\omega) \approx 1 + 2\pi n_c \gamma(q\omega) + 2\pi n_m \alpha^{q\omega} - \omega_{pm}^2/2(q\omega)^2$ $(q = 1, 3)$, where $\gamma(q\omega)$ is the cluster polarizability, $\alpha^{q\omega}$ the unionized monomer polarizability, and ω_{pm} the plasma frequency of ionized monomers. Upon ionization, $n_{\rm jet}(3\omega)$ and $n_{\rm jet}(\omega)$ diverge sharply, then partially reconverge at $\Delta t \approx 250$ fs, coincident with the delayed THG peak.

These linear optical parameters enter the expression

$$E^{3\omega}(L) = \frac{i2\pi(3\omega)^2}{c^2 k_{3\omega}} \chi^{(3)} J_{3\omega}(L) E_{\rm probe}^3, \qquad (1)$$

for the TH field via the complex phase mismatch function $J_{3\omega}(L) \equiv \frac{(e^{i\Delta kL - 3\beta^\omega L} - e^{-\beta^{3\omega} L})}{[i\Delta k - (3\beta^\omega - \beta^{3\omega})]}$ [24], plotted in Fig. 4(a), where $\Delta k = 3\omega[n_{\rm jet}(3\omega) - n_{jet}(\omega)]/c$ is the wave vector mismatch between ω and 3ω, and $\beta^{\omega,3\omega}$ extinction coefficients. $J_{3\omega}(L)$ decreases sharply from $\sim 10^{-1}$ upon ionization. Thus the ionized medium is less phase matched than the unionized clustered gas. Nevertheless, $J_{3\omega}(L)$ increases locally at $\Delta t \approx 250$ fs, when $n_{\rm jet}(3\omega)$ and $n_{\rm jet}(\omega)$ reconverge. This increase contributes to the delayed THG enhancement, but cannot by itself explain stronger THG than for the unionized medium. The calculations show $n_{\rm jet}(3\omega)$ and $n_{\rm jet}(\omega)$ could become equal at $\Delta t \approx 250$ fs, resulting in perfect phase matching, with $\sim 80\%$ clusters in the jet, possibly in a cryogenic Ar jet.

The third-order susceptibility of partially ionized clusters depends on internal gradients in ion [7,14] and/or electron [20] density, which create anharmonicity in the collective oscillation of electrons against the ion background [7,14] and/or across the internal critical surface [20], respectively. Since these gradients lie outside the framework of the uniform density model, their contribution was parametrized via an anharmonic strength $b = \varsigma \frac{\omega_p^2}{r^2}$ [7,24], where ς is a geometric constant of order unity and

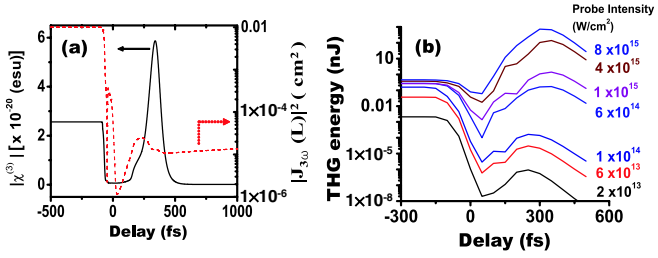

FIG. 4 (color online). Results of calculations for gas jet with 10^{18} cm^{-3} atomic density (85% monomers +15% clusters) following excitation by 10^{15} W/cm^2, 400 nm, 100 fs pump: (a) time-dependent phase-mismatch function $|J_{3\omega}(L)|^2$ (dashed curve) and $|\chi^{(3)}|$ (solid curve); (b) time-dependent THG by 800 nm probe pulses of indicated intensities.

r is a scale length ($\leq$ cluster radius r_c) of ion and/or electron density nonuniformity that was adjusted empirically to fit overall THG magnitude. The uniform density model calculated the effect of remaining material parameters on $\chi^{(3)}$, which for the complete gas jet is

$$\chi^{(3)} = \sum_{i=0}^{Z} n_{mi}\alpha_i^{(3)} + n_c \sum_{i=0}^{Z} N_i \alpha_i^{(3)} \left(\frac{3}{\varepsilon_c + 2}\right)^3 + \frac{b n_c N_e \frac{e^4}{m_e^3}}{(\omega^2 - \frac{\omega_p^2}{3} + i\nu\omega)^3[(3\omega)^2 - \frac{\omega_p^2}{3} + i\nu 3\omega]}. \quad (2)$$

The first term is the contribution of neutral ($i = 0$) and ionized ($i \geq 1$) monomers of density n_{mi}, where $\alpha_i^{(3)}$ is the atomic TH hyperpolarizability of Ar^{+i} [27]. Ionization current contributions [28] were also included. The second term is the bound electron cluster contribution, with N_i the number of neutral atoms or ions in the cluster, ε_c the cluster dielectric constant (including the contribution of neutrals, ions, and plasma [12]). Only $i = 0$ contributed significantly to the first two terms for our conditions. The third term is a generic anharmonic oscillator susceptibility describing collective oscillations of free electrons of number N_e, charge e, mass m_e inside clusters of density n_c.

The solid curve in Fig. 4(a) shows the calculated $|\chi^{(3)}|$ for $\varsigma/r^2 = 50 r_c^{-2}$, including heating and ionization by both pump and probe [29]. $|\chi^{(3)}|$ peaks at $\Delta t \approx 260$ fs, nearly simultaneously with $J_{3\omega}(L)$, where it exceeds $|\chi^{(3)}|$ prior to ionization. The parameter ς/r^2 was determined by calculating TH energy vs I_{probe}, as shown in Fig. 4(b), and adjusting ς/r^2 for best overall fit to the delayed peak. For simplicity, possible dependence of ς/r^2 on Δt or I_{probe} was not considered. Despite its simplicity, the calculation correctly reproduces the temporal evolution and growth with I_{probe} of the delayed THG peak. The fitted value of ς/r^2 correctly indicates a density nonuniformity scale length $r \ll r_c$, as required for density gradients inside a cluster. However, hydrodynamic and particle simulations will be needed to evaluate the importance of electron vs. ion density gradients, and of nonlinear electron motion driven by the ponderomotive force at the local critical surface [12,30].

In conclusion, we report delayed enhancement of THG from a noble-gas jet containing clusters that are expanding hydrodynamically in response to ultrashort pump pulse excitation. I_{probe}-dependence shows little saturation up to the pump intensity ($\sim 10^{15}$ W/cm^2). Modeling shows transient increases of cluster $\chi^{(3)}$ and phase-match factor $J_{3\omega}(L)$ both contribute to the delayed enhancement. We are currently exploring scalability of these effects to higher-order harmonic generation. For $n > 3$, enhancements of $\chi^{(n)}$ and $J_{n\omega}(L)$ are expected at earlier Δt, where probe absorption is weaker. Fully phase-matched HG may be possible up to high order ($n \sim 100$) [6] in jets with high cluster-to-monomer ratio. Delayed resonant enhancement of $\chi^{(n)}$ is expected at least up to $\alpha\omega_p^{\max} = n\omega$ [14] (i.e., $n \sim 10$ for 800 nm fundamental), and possibly higher, since resonant denominators of order $< n$ contribute to $\chi^{(n)}$. Indeed, harmonics of order $n\omega \gg \omega_p$ are observed from solid targets [2].

This work was supported by NSF Grant No. PHY-0114336 and DOE Grant No. DE-FG03-96ER40954. We thank B. Breizman, A. Arefiev, and J. Keto for useful discussions.

*Electronic address: downer@physics.utexas.edu

[1] Z. Chang *et al.*, Phys. Rev. Lett. **79**, 2967 (1997); M. Schnürer *et al.*, Phys. Rev. Lett. **80**, 3236 (1998).
[2] B. Dromey *et al.*, Nature Phys. **2**, 456 (2006).
[3] P. Agostini and L. F. DiMauro, Rep. Prog. Phys. **67**, 813 (2004); N. M. Naumova *et al.*, Phys. Rev. Lett. **92**, 063902 (2004).
[4] A. Rundquist *et al.*, Science **280**, 1412 (1998).
[5] T. D. Donnelly *et al.*, Phys. Rev. Lett. **76**, 2472 (1996).
[6] T. Tajima *et al.*, Phys. Plasmas **6**, 3759 (1999); John W. G. Tisch, Phys. Rev. A **62**, 041802(R) (2000).
[7] M. V. Fomyts'kyi *et al.*, Phys. Plasmas **11**, 3349 (2004).
[8] S. V. Fomichev *et al.*, Phys. Rev. A **71**, 013201 (2005).
[9] J. Zweiback *et al.*, Phys. Rev. A **59**, R3166 (1999).
[10] K. Y. Kim *et al.*, Phys. Rev. Lett. **90**, 023401 (2003).
[11] T. Ditmire *et al.*, Phys. Rev. A **53**, 3379 (1996).
[12] H. M. Milchberg *et al.*, Phys. Rev. E **64**, 056402 (2001).
[13] V. Kumarappan *et al.*, Phys. Rev. A **66**, 033203 (2002); V. Kumarappan *et al.*, Phys. Rev. A **67**, 043204 (2003).
[14] B. N. Breizman *et al.*, Phys. Plasmas **12**, 056706 (2005).
[15] F. Dorchies *et al.*, Phys. Rev. A **68**, 023201 (2003).
[16] I. Alexeev *et al.*, Phys. Rev. Lett. **90**, 103402 (2003); H.-H. Chu *et al.*, Phys. Rev. E **69**, 035403(R) (2004).
[17] Y. Kornyushin, Facta Universitatis. Series: Physics, Chemistry and Technology **3**, 35 (2004).
[18] H. Hamster *et al.*, Phys. Rev. Lett. **71**, 2725 (1993); T. Bartel *et al.*, Opt. Lett. **30**, 2805 (2005).
[19] Y. Fukuda *et al.*, Phys. Rev. A **73**, 031201(R) (2006).
[20] T. M. Antonsen, Jr. *et al.*, Phys. Plasmas **12**, 056703 (2005).
[21] H. M. Milchberg *et al.*, Phil. Trans. R. Soc. A **364**, 647 (2006).
[22] K. W. Madison *et al.*, Phys. Plasmas **11**, 270 (2004).
[23] E. Parra *et al.*, Phys. Rev. E **62**, R5931 (2000).
[24] Y. R. Shen, *The Principles of Nonlinear Optics* (Wiley, New York, 1984).
[25] A. Gupta *et al.*, Phys. Rev. E **70**, 046410 (2004).
[26] M. V. Ammosov *et al.*, Zh. Eksp. Teor. Fiz. **91**, 2008 (1986) [Sov. Phys. JETP **64**, 1191 (1986)].
[27] E. Dawes, Phys. Rev. **169**, 47 (1968).
[28] N. Andreev *et al.*, Sov. Phys. JETP **97**, 554 (2003).
[29] E. Springate *et al.*, Phys. Rev. A **61**, 044101 (2000).
[30] T. Taguchi *et al.*, Phys. Rev. Lett. **92**, 205003 (2004).